Interaction of three regiospecific amino acid residues is required for OATP1B1 gain of OATP1B3 substrate specificity

Marianne K. DeGorter
Western University

Richard H. Ho
Vanderbilt University Medical Center

Brenda F. Leake
Vanderbilt University Medical Center

Rommel G. Tirona
Western University, rommel.tirona@schulich.uwo.ca

Richard B. Kim
Western University, richard.kim@lhsc.on.ca

Interaction of three regio-specific amino acid residues is required for OATP1B1 gain of OATP1B3 substrate specificity

Marianne K. DeGorter[a,b], **Richard H. Ho**[c], **Brenda F. Leake**[d], **Rommel G. Tirona**[a,b], and **Richard B. Kim**[a,b,*]

[a]Department of Physiology and Pharmacology, University of Western Ontario, London, Ontario, Canada

[b]Division of Clinical Pharmacology, Department of Medicine, University of Western Ontario, London, Ontario, Canada

[c]Department of Pediatrics, Vanderbilt University Medical Center, Nashville, Tennessee

[d]Division of Clinical Pharmacology, Vanderbilt University Medical Center, Nashville, Tennessee

Abstract

The human organic anion-transporting polypeptides OATP1B1 (*SLCO1B1)* and OATP1B3 *(SLCO1B3)* are liver-enriched membrane transporters of major importance to hepatic uptake of numerous endogenous compounds including bile acids, steroid conjugates, hormones, and drugs including the 3-hydroxy-3-methylglutaryl Co-A reductase inhibitor (statin) family of cholesterol-lowering compounds. Despite their remarkable substrate overlap, there are notable exceptions: in particular, the gastrointestinal peptide hormone cholecystokinin-8 (CCK-8) is a high affinity substrate for OATP1B3 but not OATP1B1. We utilized homologous recombination of linear DNA by *E. coli* to generate a library of cDNA containing monomer size chimeric OATP1B1-1B3 and OATP1B3-1B1 transporters with randomly distributed chimeric junctions to identify three discrete regions of the transporter involved in conferring CCK-8 transport activity. Site-directed mutagenesis of three key residues in OATP1B1 transmembrane helices 1 and 10, and extracellular loop 6, to the corresponding residues in OATP1B3, resulted in a gain of CCK-8 transport by OATP1B1. The residues appear specific to CCK-8, as the mutations did not affect transport of the shared OATP1B substrate atorvastatin or the OATP1B1-specific substrate estrone sulfate. Regions involved in gain of CCK-8 transport by OATP1B1, when mapped to the crystal structures of bacterial transporters from the major facilitator superfamily, suggest these regions could readily interact with drug substrates. Accordingly, our data provide new insight into the molecular determinants of the substrate specificity of these hepatic uptake transporters with relevance to targeted drug design and prediction of drug-drug interactions.

Keywords

hepatic uptake transport; organic anion transporting polypeptide; site-directed mutagenesis

Introduction

The organic anion-transporting polypeptides (OATPs; gene symbol solute carrier family *SLCO*) form a superfamily of transmembrane proteins involved in the transport of a variety of amphipathic substrates across the plasma membrane in a sodium-independent manner. To date, over 80 members of the OATP superfamily in 13 different species have been identified by the presence of the OATP superfamily signature D-X-RW-(I,V)-GAWW-X-G-(F,L)-L. The two members of the human subfamily OATP1B, OATP1B1 (previously known as OATP-C, liver-specific transporter 1 (LST-1), or OATP2; gene symbol *SLCO1B1*, previously *SLC21A6*) and OATP1B3 (previously known as LST-2, or OATP8; gene symbol *SLCO1B3*, previously *SLC21A8*), share 80% sequence identity[1]. Their expression is predominantly observed on the basolateral membrane of hepatocytes, where they mediate the hepatic uptake of substrates from the portal blood[2–5]. Not surprisingly, OATP1B1 and OATP1B3 share a broad substrate specificity, and are capable of transporting bile salts, steroid conjugates, the thyroid hormones T3 and T4, eicosanoids, cyclic peptides, bromosulfophthalein, the natural toxins phalloidin and microcystin-LR as well as numerous drugs, such as methotrexate, rifampin, and many of the 3-hydroxy-3-methylglutaryl coenzyme A (statin) family of compounds[1, 6–8].

Reports of mice with deletion of Oatp1b2 (*Slco1b2)*, the closest murine ortholog to OATP1B1 and OATP1B3, observed altered pharmacokinetic profiles of prototypical OATP1B1 substrates pravastatin and rifampin[9], as well as protection from hepatotoxicity induced by phalloidin and microcystin-LR[10]. The clinical relevance of OATP1B1 to hepatic elimination is also evidenced by the profound effect of single nucleotide polymorphisms (SNPs) on the observed pharmacokinetic profile of drug substrates[7]. Remarkably, a previously identified SNP in *SLCO1B1* has been shown to be the single most important predictor of statin-induced muscle myopathy, a relatively rare but potentially fatal side effect of statin therapy[11–12].

Despite their remarkable sequence similarity and overlapping substrate specificity, there are some notable differences in the compounds transported by OATP1B1 and OATP1B3. For example, OATP1B3 transports the gastrointestinal peptide hormone cholecystokinin-8 (CCK-8), which is not a substrate of OATP1B1[1, 13–14]. Conversely, OATP1B1 transports the steroid conjugate estrone sulfate while OATP1B3 does not show appreciable transport activity. Accordingly, the wide and overlapping but not identical substrate specificity of OATP1B1 and OATP1B3, combined with their significant sequence homology, suggests that there may be key sequence differences that confer isoform-specific divergence in substrate specificity.

Previously, transmembrane (TM) helices eight and nine were identified as important for estrone sulfate and estradiol-17β-glucuronide transport by OATP1B1[15], and the mutation of four residues in TM10, Leu[545], Phe[546], Leu[550] and Ser[554], resulted in complete loss of estrone sulfate transport[16]. Conserved, positively charged amino acids in other areas of OATP1B1 also appear to be important for estrone sulfate and estradiol-17β-glucuronide transport[17]. With respect to OATP1B3, previous studies have indicated a role for TM10 in mediating CCK-8 transport[18]. Similar to OATP1B1, conserved, positively charged amino acids in OATP1B3 appear to be important for transport of sulphobromophthalein (BSP), pravastatin and taurocholate[19–20].

Given the importance of OATP1B1 in hepatic drug uptake, the molecular basis for substrate specificity needs to be defined to more fully understand the in vivo distribution of its substrates, and to aid in the rational design of drugs targeting the liver as their site of action. In the present work, we employed a strategy of random chimeragenesis to obtain insight to

specific regions involved in CCK-8 transport. Our results indicate that amino acid residues in three distinct regions of the transporter are required to enable CCK-8 transport by OATP1B3. Importantly, we were able to confer CCK-8 transport by OATP1B1 through targeted mutagenesis of amino acids in the regions noted to be important for CCK-8 transport by OATP1B3.

Experimental Section

Materials

[³H]-CCK-8(L-aspartyl-L-tryosyl-L-methionylgylcyl-L-tryptophyl-L-methionyl-L-aspartyl-L-phenylalaninamide hydrogen sulfate ester; 93 Ci/mmol, >97% purity) was purchased from GE Healthcare (Buckinghamshire, UK), [³H]-estrone sulfate (57.3 Ci/mmol, >97% purity) from PerkinElmer (Boston, MA), and [³H]-atorvastatin (5 Ci/mmol, >97% purity) from American Radiolabeled Chemicals (St Louis, MO). Unlabeled estrone sulfate was from Sigma-Aldrich (St. Louis, MO), atorvastatin was from Toronto Research Chemicals (North York, Canada) and cholecystokinin-8 was from Bachem Bioscience (King of Prussia, PA).

OATP1B chimera plasmid construct

The master plasmids for chimeragenesis were created by inserting the coding sequence of OATP1B1 into a previously described pEF6/V5-His TOPO plasmid containing OATP1B3[21]. Two master plasmids with the transporters in a tandem head-to-tail arrangement were created: OATP1B1-1B3 and OATP1B3-1B1. OATP1B1 was released from pEF6[12] by PCR using the Phusion® High Fidelity PCR kit (New England Biolabs, Ipswich, MA), with primers that introduced restriction enzymes sites to allow insertion of OATP1B1 into the multiple cloning regions of pEF6-OATP1B3. For OATP1B1-1B3, OATP1B1 was released using the forward primer 5'-ggatccacta gtccagtgtg gtggaattgc ccttgatatc tatatttcaa-3' and the reverse primer 5'-tctagac**act** ag**t**ggccg**tt aac**gtgctg**c** atat**g**tgcag aattgccctt ttaacaatgt-3', with nucleotides mutated to add *Hpa*I, *Nde*I and *Spe*I restriction sites in bold. The resulting fragment was ligated into pEF-OATP1B3 using *Spe*I and the orientation of the fragment was confirmed by restriction digest (Fig. 1A). For OATP1B3-1B1, the forward primer 5' – gtccagtg**cg** g**ccgc**attgc c**att**t**aa**atc tatatttcaa ccatggacca – 3' to add *Not*I and *Swa*I sites and reverse primer 5' – gccactgt gctggatatc t**ct**agaattg ccctttaac aatgtgt – 3' to add *Xba*I sites were used. The resulting fragment was ligated into pEF-OATP1B3 using *Not*I and *Xba*I (Fig. 1B). The resulting master plasmids OATP1B1-1B3 and OATP1B3-1B1 were linearized by *Hpa*I and *Nde*I, and *Not*I and *Swa*I respectively, and inserted into TOP10 *Escherichia coli* (Invitrogen, Carlsbad, CA). Restriction fragments resulting from digesting the ensuing plasmids with *Spe*I and *Xba*I were used to select those plasmids containing a monomeric OATP1B sequence. OATP1B1-specific restriction enzymes were used to estimate the approximate location of the junction between OATP1B1 and OATP1B3; sequencing determined the exact location of the junction.

Site-directed mutagenesis

Single, double and triple point mutations were introduced into the coding sequence of pEF6-OATP1B1 and pEF6-OATP1B3 using the QuikChange® Multi Site-directed Mutagenesis kit (Stratagene, La Jolla, CA) according to the manufacturer's instructions. The primers used are summarized in SI Table 1. The presence of all mutations was confirmed by sequencing.

Transient transfection and transport assay

HeLa cells were plated in 12-well plates at 2.5×10^5 cells/well, to be transfected the next day. Transporters were expressed using a transient heterologous expresssion system as previously described[12]. Briefly, 750 ng cDNA per well as measured by PicoGreen® Assay

(Invitrogen) with Lipofectin® (Invitrogen) in Opti-MEM® (Lonza, Walkersville, MD). Sixteen hours later, the cells were washed in pre-warmed Opti-MEM (CCK-8) or Krebs Henseleit Bicarbonate (KHB) buffer (estrone sulfate and atorvastatin; 1.2 mM $MgSO_4$, 0.96 mM KH_2PO_4, 4.83 mM KCl, 118 mM NaCl, 1.53 mM $CaCl_2$, 23.8 mM $NaHCO_3$, 12.5 mM HEPES, 5 mM glucose, pH 7.4), then dosed with 400 μl Opti-MEM or KHB buffer containing radiolabeled substrates and varying concentrations of unlabeled compounds, and incubated at 37 °C. Chimeric transporters and OATP1B1 mutants screened for CCK-8 transport activity (2 nM) were incubated for 30 min. Kinetics experiments measuring uptake by the triple mutants were conducted at 10 min, within the linear uptake phase of CCK-8 by OATP1B3. Estrone sulfate uptake (100 nM) was measured after 5 min incubation, atorvastatin uptake (75 nM) was measured after 10 min. Cells were washed three times in ice-cold PBS, harvested in 500 μl 1% SDS, and radioactivity was measured by scintillation counting. Specific uptake was determined by subtracting uptake by vector-transfected control from the total measured. Percent OATP1B3 uptake was calculated by dividing the specific uptake of a chimeric or mutated transporter by the specific uptake of CCK-8 by wild-type OATP1B3 during the same experiment. Statistical determination of differences was by analysis of variance, with Dunnett's multiple comparison test, and student's t-test as appropriate. Kinetic parameters K_m and V_{max} were calculated by Michaelis-Menten non-linear curve fitting (GraphPad Prism, San Diego, CA).

Cell surface expression and immunoblots

Cell surface biotinylation was carried out as previously described[12] to determine the extent of cell surface trafficking of heterologously expressed transporters. Briefly, Hela cells (~ 8 × 10^5 cells/well) were transfected as described for transport experiments. Sixteen hours post-transfection, the cells were washed in ice-cold PBS-Ca^{2+}/Mg^{2+} (138 mM $NaCl_2$, 2.7mM KCl, 1.5 mM KH_2PO_4, 1mM $MgCl_2$, 0.1 mM $CaCl_2$, pH 7.3) and treated with sulfo-N-hydroxysuccinimide-SS-biotin (Thermo Scientific, Rockford, IL). The cells were washed with ice-cold PBS-Ca^{2+}/Mg^{2+} containing 100 mM glycine and disrupted with lysis buffer (10 nM Tris base, 150 mM NaCl, 1 mM EDTA, 0.1% SDS, 1% Triton X-100, pH 7.4) containing protease inhibitors (Complete, Roche Applied Science, Indianapolis, IN). Following centrifugation, 140 μl of streptavidin-agarose beads (Thermo Scientific, Rockford, IL) were added to 600 μl of cell lysate, and incubated for one hour at room temperature. Beads were washed four times with ice-cold lysis buffer, and biotinylated proteins released from the beads by adding Laemmli buffer. Biotinylated (cell surface-expressed) fractions and total cell lysates (25μl) were subjected to Western blotting analysis for detection of OATP1B1 or OATP1B3 by specific polyclonal antibodies as previously described[12]. The intracellular, endoplasmic reticulum-resident protein calnexin was probed as a loading control (1:2000 dilution, StressGen,Victoria, British Columbia, Canada). Densitometry analysis was performed using ImageJ (http://imagej.nih.gov/ij/).

Results

[³H]-CCK-8 uptake by transfected cells expressing OATP1B1-1B3 and OATP1B3-1B1 chimeras identifies regions in TM1, TM10 and extracellular loop 6 (ECL6) involved in CCK-8 transport

A library of OATP1B1-1B3 and OATP1B3-1B1 chimeric expression constructs was generated using homologous recombination of linear DNA by *E. coli*. Sequencing of the constructs indicated that the chimeric junctions were well distributed throughout the coding sequence (Fig. 2). Screening of the chimeras for transport of CCK-8 identified three regions of interest defined by the overlap of sequences causing altered transport activity in both sets of chimeras. A substantial decrease in CCK-8 transport by OATP1B1-1B3 chimeras with junctions at Gly[26] and Phe[59] combined with a modest increase by OATP1B3-1B1 chimeras

with junctions at Ser[35] and Cys[101] forms a region of interest between Ser[35] and Phe[59]. This region is located close to the predicted extracellular boundary of transmembrane helix 1 (TM1). A second region of interest is formed by a change in transport activity in OATP1B1-1B3 chimeras with junctions at Phe[534] and Asp[596], and OATP1B3-1B1 chimeras with junctions at Tyr[481] and Lys[568], creating a region of interest between Phe[534] and Lys[568]. A third region is formed by the overlap of a region responsible for a significant gain in OATP1B3-1B1 transport in chimeras with junctions at Gly[608] and Gln[652] with a small but detectable decrease in CCK-8 transport in OATP1B1-1B3 chimeras with junctions at Asp[596] and Ser[629]. This region, defined by Gly[608] and Ser[629], is located in a portion of the predicted extracellular loop (ECL) 6 close to TM12. Within these regions, seven non-conserved amino acids in both TM1 and ECL6 and twelve non-conserved residues in TM10 were mutated in OATP1B1 to the corresponding residue in OATP1B3.

Site-directed mutagenesis of non-conserved residues indicates amino acids at positions 45 in TM1, 545 in TM10 and 615 in ECL 6 near TM12 contribute to CCK-8 transport

OATP1B1 mutants of nonconserved residues in OATP1B3 located in the region of TM1 defined by the chimeras were created by site-directed mutagenesis and screened for CCK-8 transport (Fig. 3). Of the seven mutants created, L36F, F38Y, T42A, A45G, S50I, I53T and H54Q, the OATP1B1 mutant A45G showed the greatest transport activity, at 0.8% of wildtype OATP1B3 CCK-8 transport, compared with 0.3% activity normally observed for wildtype OATP1B1 (Fig. 3B; $p < 0.01$). The corresponding mutation of OATP1B3 to the OATP1B1 residue, OATP1B3 G45A, exhibited approximately a 35% decrease in CCK-8 transport compared to wildtype OATP1B3 (Fig. 3E; $p < 0.001$).

In the region of TM10 defined by the chimeric transporters, a total of 12 OATP1B1 mutants were created: Y535F, F536I, F537Y, L543I, L545S, F546L, L550T, S554T, H555F, V556I, M557L, and I559T (Fig. 3D). Of the mutations in this region, OATP1B1 L545S exhibited the highest level of CCK-8 transport, at 0.8% of wildtype OATP1B3 ($p < 0.01$). Approximately 16% of wild CCK-8 transport was observed by the corresponding mutation OATP1B3 S545L (Fig. 3E; $p < 0.001$).

Finally, of seven OATP1B1 mutants in ECL6, T609A, R610Q, S612A, T615I, T619V, S620F and S622G, the OATP1B1 mutant T615I exhibited the greatest increase in CCK-8 transport over wildtype OATP1B1 transport, to 1.5% of OATP1B3 transport activity ($p < 0.001$). The corresponding mutation, OATP1B3 I615T, showed a close to 55% decrease in transport activity (Fig. 3E; $p < 0.001$).

To investigate the potential for interactions between two or more regions identified by the chimeric transporters to be involved in CCK-8 transport, the double mutants OATP1B1 A45G/L545S, OATP1B1 L545S/T615I, and OATP1B1 A45G/T615I were constructed. The double mutants exhibited 3.9, 2.2 and 2.9 % of OATP1B3 CCK-8 uptake, respectively (Fig. 5A). Similarly, the double mutants OATP1B3 G45A/S545L, OATP1B3 S545L/I615T and OATP1B3 G45A/I615T exhibited a marked, but not total, loss of CCK-8 transport activity (Fig. 5C).

In contrast, when a mutation from each of the three regions identified by the chimeric transporters were combined in the triple mutant OATP1B1 A45G/L545S/T615I, a profound gain of CCK-8 transport activity was observed, corresponding to 16% of wildtype OATP1B3 CCK-8 uptake (Fig. 5B; $p < 0.001$). The corresponding triple mutant OATP1B3 G45A/S545L/I615T exhibited almost complete abrogation of CCK-8 transport (Fig. 5D; $p < 0.001$).

Cell surface biotinylation studies were conducted to examine whether the observed changes in transport activity were related to cell surface expression of the transporter. Western blot analysis indicates that there is no significant difference in cell surface expression in those OATP1B1 mutants with altered CCK-8 transport activity (Fig. 4A, 4C), suggesting that the increase in CCK-8 transport activity observed is due to altered substrate recognition or transport capacity, and does not appear to be a result of changed levels of cell surface expressed transporter. On the other hand, reduced cell surface expression of OATP1B3 G45A/S545L/I615T may partially account for the loss of CCK-8 transport, though it is important to note that the mutant cell surface expression is approximately 40% of wildtype, suggesting that the protein is not capable of CCK-8 transport (Fig 4D).

Characterization of CCK-8 transport kinetics of OATP1B1 triple mutant and wildtype OATP1B3

The kinetics of CCK-8 uptake by the OATP1B1 triple mutant A45G/L545S/T615I compared to wildtype OATP1B3 were examined by measuring [^{3}H]-CCK-8 uptake after 10 minutes in the presence of unlabeled CCK-8 varying in concentration from 2 nM to 100 μM. Results indicate a higher K_m (15.4 ± 4.2 μM vs. 6.5 ± 2.0 μM) and a lower V_{max} (0.020 ± 0.0018 nmol/mg protein/min vs. 0.064 ± 0.0049 nmol/mg protein/min) for the OATP1B1 triple mutant compared to wildtype OATP1B3 uptake (Fig. 6). V_{max} and K_m for the OATP1B1-mediated uptake of CCK-8 were undeterminable. Intrinsic clearance values (V_{max}/K_m) were lower in the OATP1B1 triple mutant (1.2 μl/mg protein/min) compared to wildtype OATP1B3 (9.8 μl/mg protein/min), due to the lower V_{max} and higher K_m of the OATP1B1 triple mutant.

Transport of other OATP1B substrates by OATP1B1 and OATP1B3 triple mutants

The OATP1B1-specific substrate estrone sulfate was not transported by wildtype OATP1B3 or the OATP1B3 triple mutant G45A/S545L/I615T (Fig. 7A). Transport of estrone sulfate by the OATP1B1 triple mutant A45G/L545S/T615I was reduced to approximately 50% of uptake by wildtype OATP1B1. Transport of the shared OATP1B substrate atorvastatin was modestly increased by OATP1B1 A45G/L545S/T615I and modestly reduced by OATP1B3 G45A/S545L/I615T, compared to their respective wildtype transporters (Fig. 7B,C).

Discussion

The molecular basis for the substrate specificity and transport activity of the OATP superfamily is not well understood, despite that OATP transporters are increasingly recognized as important determinants of interindividual variation in response to many drugs in clinical use[7]. Transport by the OATPs appears to be mediated by a Na^+-independent and electroneutral process, but the precise details of the transport mechanism, including the identity of the counterion, remain to be elucidated. Hydropathy analysis of OATP/Oatp sequences indicates that members of the superfamily form 12 TMs with intracellular amino- and carboxy termini, an arrangement that was shown experimentally for the murine transporter oatp1a1[22]. The OATPs have in common a large predicted ECL5 between TMs 9 and 10; characterization of conserved cysteine residues in ECL5 of OATP2B1 indicate these residues are involved in membrane trafficking and transport function[23]. Other conserved features include N-glycosylation sites in ECLs 2 and 5, and the superfamily signature that designates the OATP family, found at the border between ECL3 and TM6[24].

CCK-8 is a gastrointestinal peptide hormone released postprandially in response to nutrients in the gut, and is involved in delaying gastric emptying, as well as stimulating pancreatic enzyme secretion, gall bladder contraction and intestinal motility[25]. Interestingly, CCK-8 appears to be transported by OATP1B3 but not by the closely related OATP1B1. The main

goal of our current study was to identify key regions or amino acid residues which could confer gain of CCK-8 transport function for OATP1B1.

We first noted that chimeras from each set sharing the same junction close to middle of transporter (Val[339]), OATP1B3-1B1-6, and OATP1B1-1B3-9, demonstrated a modest gain or significant loss of wildtype OATP1B3 CCK-8 transport, respectively, compared to adjacent chimeras (Fig. 2). OATP1B1-1B3-9 demonstrated higher CCK-8 transport activity than OATP1B3-1B1-6 (Fig. 2), consistent with other reports that the C-terminal portion of OATP1B3 is more important for CCK-8 transport than the N-terminal portion[18]. Systematic comparison of the individual chimeric transporter function suggested that amino acids in TM1, TM10, and ECL6 may be important for CCK-8 transport. Given the two negatively charged aspartic acid residues in CCK-8, it might be expected that there exists some critical interaction with positively charged residues in the transporter, especially given the importance of positively charged residues to OATP1B3 transport of other substrates[19–20]. However, none of the OATP1B1 mutations made were to a positively charged residue in OATP1B3. Three nonconserved positively charged residues in OATP1B1 were substituted for an uncharged residue at the corresponding position in OATP1B3, however, none of the three variants, H54Q, H555F or R610Q, showed any significant increase in CCK-8 transport (Fig. 3B, 3C and 3D). In total five aromatic residues, Phe[38], Tyr[535], Phe[536], Phe[537] and Phe[546] in OATP1B1 fell within the regions identified, and were mutated to the corresponding residue in OATP1B3. At three of these positions, the mutation was a semi-conserved mutation to a different aromatic residue (F38Y, Y535F and F537Y). In three other positions, non-aromatic residues in OATP1B1 were converted to aromatic side chains: L36F, H555F and S620F. The absence of any significant gain of function in any of these OATP1B1 mutations suggests that these residues may not be involved in the CCK-8 transport cycle.

The mutation of an alanine at position 45 to glycine in TM1 of OATP1B1 resulted in an increase in CCK-8 transport. It is possible this may be attributed to the loss of bulk of the methyl group difference between these two side chains, a consideration particularly given that CCK-8 is a relatively large substrate. Mutation of OATP1B1 from a leucine to a serine at position 545 adds a hydroxyl group, in addition to reducing the bulk associated with the side chain, while the mutation of threonine at position 615 to isoleucine results in a loss of a hydroxyl group. This suggests a possible role for the interaction of a hydroxyl group with CCK-8 in a way that either promotes or prevents CCK-8 transport. It is also possible that the mutations noted alter protein conformation in a way that affects substrate specificity without directly interacting with CCK-8.

A previous report that utilized a TM domain swapping strategy indicated the importance of TM10 in CCK-8 transport by OATP1B3[18]. It should be noted that the study by Gui and Hagenbuch focused on the substitution of individual transmembrane spanning domains in OATP1B3 with the corresponding TMs of OATP1B1. Accordingly, their study was designed to detect a loss of CCK-8 transport due to the presence of an OATP1B1-specific TM region. In the current study, we pursued a chimeragenesis approach to generate a library of both OATP1B1-1B3 and OATP1B3-1B1 monomer sized chimeras to identify chimeric junctions that revealed a gain and corresponding loss of function, without an a priori bias regarding the overall importance of TM regions versus intracellular or extracellular loops in the transporter. Although our data confirms TM10 is a key region for CCK-8 interaction, mutation of a single residue in TM10 is not sufficient to impart a true gain of OATP1B1-mediated CCK-8 transport (Fig. 3D). Indeed our current data reveals that the synergistic interaction with two additional domains is essential. Although it should be noted that the overall activity of the OATP1B1 45/545/615 triple mutant was lower than that of the wildtype OATP1B3, it is remarkable that three targeted amino acid substitutions changed

OATP1B1 from complete inability to transport CCK-8 to attaining near 15% of OATP1B3 activity (Fig. 5B). Conversely, substitution of amino acids at those positions in OATP1B3 to the corresponding residue in OATP1B1 resulted in the near complete loss of OATP1B3-mediated CCK-8 uptake (Fig. 5D), despite the fact this mutant is expressed on the cell surface, albeit at lower levels than wildtype OATP1B3 (Fig. 4D).

The three key amino acid residues noted for CCK-8 gain of substrate specificity do not appear to confer the opposite effect, that is, OATP1B3 gain of function for an OATP1B1-specific substrate such as estrone sulfate (Fig. 7A). Similarly, there was not a readily discernible effect of the three amino acid residues on the transport of the shared (OATP1B1 and OATP1B3) substrate and commonly prescribed statin, atorvastatin (Fig. 7B,C). Therefore it seems the amino acids we have identified in this study, though key residues with respect to CCK-8 transport, are not essential to conferring OATP1B1-specific or OATP1B1 and 1B3 shared substrate specificity. This is consistent with a recent report that TM8 and TM9 of OATP1B1 are involved in the transport of its steroid conjugate substrates estrone sulfate and estradiol glucuronide[15].

Like other transporters, little structural data for the OATPs exists due to challenges associated with the purification and crystallization of large membrane-bound structures. A homology model for OATP1B3 based on the crystal structures of the glycerol-3-phosphate transporter and lactose permease from *E. coli* has been reported[26–28]. More recently, the structure of the multidrug transporter EmrD from *E. coli* has been used to model OATP1B3[18, 29]. There appears to be significant structural conservation in the major facilitator superfamily (MFS) of transporters[30], so these crystal structures from bacteria may serve as models to interpret data arising from functional characterization of the distantly related OATPs. In each of the three MFS structures mentioned it appears that both TM1 and TM10 partially form the pore of the transporter, consistent with the biochemical data presented here to suggest that these regions are involved in CCK-8 transport (Fig. 8).

This study is important to the drug development process for a number of reasons. The exclusive expression of OATP1B1 on the basolateral membrane of hepatocytes makes it an attractive target for drugs requiring entry into the liver in order to exert their effect. Species differences in OATP expression in the liver and other organs adds complexity to studying human OATPs and mean that in vitro and in silico approaches may prove useful in predicting the in vivo activity of human OATPs. In addition to species differences in substrate specificity, there are zonal differences in OATP expression within a given tissue. In particular, OATP1B1 is expressed in hepatocytes throughout the liver, while OATP1B3 is expressed primarily in the perivenous hepatocytes, indicating there are important differences in transporter regulation[31]. Thus targeting one OATP over another has the potential to result in even greater tissue specificity.

Finally, given the importance of OATPs to the cellular uptake of many drugs, it will be useful to have the ability to predict the functional effect of novel polymorphisms in OATPs that will be discovered as whole genome sequencing expands into clinical applications. At the time of this writing, there was only one reported case of a naturally occurring polymorphism in any of the same positions as the 26 mutations in OATP1B1 presented here, Leu543Trp (rs72661137). It remains difficult to predict the precise effect of a polymorphism in OATP1B1, however, there was a modest increase in CCK-8 transport by the Leu543Ile mutant in our study (Fig 3D). Given this, combined with its proximity to the Leu545 residue identified here to be important for CCK-8 transport, we believe it is not unreasonable to expect that Leu543 polymorphisms may alter OATP1B1 function, and further studies of this polymorphism may be warranted.

In conclusion, hepatic uptake transporters are increasingly recognized as important determinants of drug disposition and response. Accordingly, substrate recognition by OATP1B1 and OATP1B3 may be an important consideration for predicting potential transporter mediated drug interactions and rational drug design. Indeed substrate specificity of OATP1B1 and OATP1B3 may also provide valuable information for enhancing liver-to-plasma ratio in the design of compounds targeted to the liver. This report is the first to identify three amino acids, 45 (TM1), 545 (TM10) and 615 (ECL6) in distinct regions of the transporter interact to confer gain of function of transport of CCK-8 by OATP1B1. This data contributes new insight to our understanding of substrate specificity in these important hepatic transporters.

Supplementary Material

Refer to Web version on PubMed Central for supplementary material.

Acknowledgments

References

1. Hagenbuch B, Meier PJ. Organic anion transporting polypeptides of the OATP/ SLC21 family: phylogenetic classification as OATP/ SLCO superfamily, new nomenclature and molecular/ functional properties. Pflugers Arch. 2004; 447(5):653–65. [PubMed: 14579113]

2. Abe T, Kakyo M, Tokui T, Nakagomi R, Nishio T, Nakai D, Nomura H, Unno M, Suzuki M, Naitoh T, Matsuno S, Yawo H. Identification of a novel gene family encoding human liver-specific organic anion transporter LST-1. J Biol Chem. 1999; 274(24):17159–63. [PubMed: 10358072]

3. Konig J, Cui Y, Nies AT, Keppler D. A novel human organic anion transporting polypeptide localized to the basolateral hepatocyte membrane. Am J Physiol Gastrointest Liver Physiol. 2000; 278(1):G156–64. [PubMed: 10644574]

4. Hsiang B, Zhu Y, Wang Z, Wu Y, Sasseville V, Yang WP, Kirchgessner TG. A novel human hepatic organic anion transporting polypeptide (OATP2). Identification of a liver-specific human organic anion transporting polypeptide and identification of rat and human hydroxymethylglutaryl-CoA reductase inhibitor transporters. J Biol Chem. 1999; 274(52):37161–8. [PubMed: 10601278]

5. Konig J, Cui Y, Nies AT, Keppler D. Localization and genomic organization of a new hepatocellular organic anion transporting polypeptide. J Biol Chem. 2000; 275(30):23161–8. [PubMed: 10779507]

6. Glaeser H, Bailey DG, Dresser GK, Gregor JC, Schwarz UI, McGrath JS, Jolicoeur E, Lee W, Leake BF, Tirona RG, Kim RB. Intestinal drug transporter expression and the impact of grapefruit juice in humans. Clin Pharmacol Ther. 2007; 81(3):362–70. [PubMed: 17215845]

7. Tirona, RG.; Kim, RB. Organic Anion-transporting Polypeptides. In: You, G.; Morris, ME., editors. Drug Transporters. John Wiley & Sons, Inc; Hoboken, NJ: 2007. p. 75-104.

8. Hagenbuch B, Gui C. Xenobiotic transporters of the human organic anion transporting polypeptides (OATP) family. Xenobiotica. 2008; 38(7–8):778–801. [PubMed: 18668430]

9. Zaher H, zu Schwabedissen HE, Tirona RG, Cox ML, Obert LA, Agrawal N, Palandra J, Stock JL, Kim RB, Ware JA. Targeted disruption of murine organic anion-transporting polypeptide 1b2 (Oatp1b2/Slco1b2) significantly alters disposition of prototypical drug substrates pravastatin and rifampin. Mol Pharmacol. 2008; 74(2):320–9. [PubMed: 18413659]

10. Lu H, Choudhuri S, Ogura K, Csanaky IL, Lei X, Cheng X, Song PZ, Klaassen CD. Characterization of organic anion transporting polypeptide 1b2-null mice: essential role in hepatic uptake/toxicity of phalloidin and microcystin-LR. Toxicol Sci. 2008; 103(1):35–45. [PubMed: 18296417]
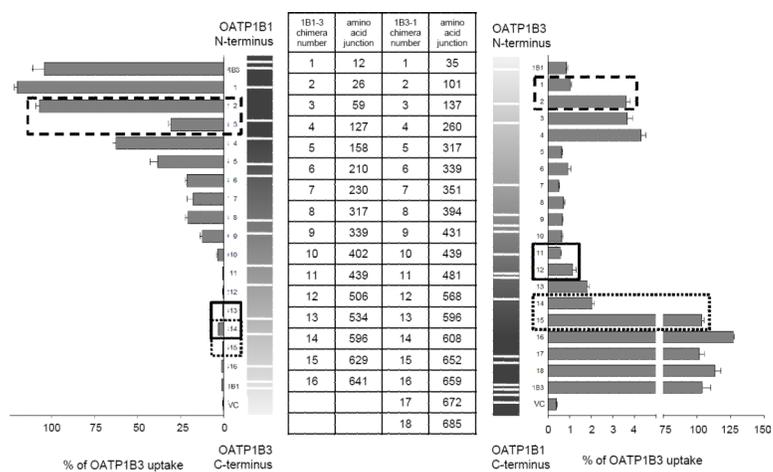
11. Link E, Parish S, Armitage J, Bowman L, Heath S, Matsuda F, Gut I, Lathrop M, Collins R. SLCO1B1 variants and statin-induced myopathy--a genomewide study. N Engl J Med. 2008; 359(8):789–99. [PubMed: 18650507]

12. Tirona RG, Leake BF, Merino G, Kim RB. Polymorphisms in OATP-C: identification of multiple allelic variants associated with altered transport activity among European- and African-Americans. J Biol Chem. 2001; 276(38):35669–75. [PubMed: 11477075]

13. Ismair MG, Stieger B, Cattori V, Hagenbuch B, Fried M, Meier PJ, Kullak-Ublick GA. Hepatic uptake of cholecystokinin octapeptide by organic anion-transporting polypeptides OATP4 and OATP8 of rat and human liver. Gastroenterology. 2001; 121(5):1185–90. [PubMed: 11677211]

14. Ishiguro N, Maeda K, Kishimoto W, Saito A, Harada A, Ebner T, Roth W, Igarashi T, Sugiyama Y. Predominant contribution of OATP1B3 to the hepatic uptake of telmisartan, an angiotensin II receptor antagonist, in humans. Drug Metab Dispos. 2006; 34(7):1109–15. [PubMed: 16611857]

15. Miyagawa M, Maeda K, Aoyama A, Sugiyama Y. The eighth and ninth transmembrane domains in organic anion transporting polypeptide 1B1 affect the transport kinetics of estrone-3-sulfate and estradiol-17beta-D-glucuronide. J Pharmacol Exp Ther. 2009; 329(2):551–7. [PubMed: 19244099]

16. Gui C, Hagenbuch B. Role of transmembrane domain 10 for the function of organic anion transporting polypeptide 1B1. Protein Sci. 2009; 18(11):2298–306. [PubMed: 19760661]

17. Weaver YM, Hagenbuch B. Several conserved positively charged amino acids in OATP1B1 are involved in binding or translocation of different substrates. J Membr Biol. 2010; 236(3):279–90. [PubMed: 20821001]

18. Gui C, Hagenbuch B. Amino acid residues in transmembrane domain 10 of organic anion transporting polypeptide 1B3 are critical for cholecystokinin octapeptide transport. Biochemistry. 2008; 47(35):9090–7. [PubMed: 18690707]

19. Glaeser H, Mandery K, Sticht H, Fromm MF, Konig J. Relevance of conserved lysine and arginine residues in transmembrane helices for the transport activity of organic anion transporting polypeptide 1B3. Br J Pharmacol. 2010; 159(3):698–708. [PubMed: 20100277]

20. Mandery K, Sticht H, Bujok K, Schmidt I, Fahrmayr C, Balk B, Fromm MF, Glaeser H. Functional and structural relevance of conserved positively charged lysine residues in organic anion transporting polypeptide 1B3. Mol Pharmacol. 2011

21. Tirona RG, Leake BF, Wolkoff AW, Kim RB. Human organic anion transporting polypeptide-C (SLC21A6) is a major determinant of rifampin-mediated pregnane X receptor activation. J Pharmacol Exp Ther. 2003; 304(1):223–8. [PubMed: 12490595]

22. Wang P, Hata S, Xiao Y, Murray JW, Wolkoff AW. Topological assessment of oatp1a1: a 12-transmembrane domain integral membrane protein with three N-linked carbohydrate chains. Am J Physiol Gastrointest Liver Physiol. 2008; 294(4):G1052–9. [PubMed: 18308854]

23. Hanggi E, Grundschober AF, Leuthold S, Meier PJ, St-Pierre MV. Functional analysis of the extracellular cysteine residues in the human organic anion transporting polypeptide, OATP2B1. Mol Pharmacol. 2006; 70(3):806–17. [PubMed: 16754786]

24. Hagenbuch B, Meier PJ. The superfamily of organic anion transporting polypeptides. Biochim Biophys Acta. 2003; 1609(1):1–18. [PubMed: 12507753]

25. Wren AM, Bloom SR. Gut hormones and appetite control. Gastroenterology. 2007; 132(6):2116–30. [PubMed: 17498507]

26. Abramson J, Smirnova I, Kasho V, Verner G, Kaback HR, Iwata S. Structure and mechanism of the lactose permease of Escherichia coli. Science. 2003; 301(5633):610–5. [PubMed: 12893935]

27. Meier-Abt F, Mokrab Y, Mizuguchi K. Organic anion transporting polypeptides of the OATP/SLCO superfamily: identification of new members in nonmammalian species, comparative modeling and a potential transport mode. J Membr Biol. 2005; 208(3):213–27. [PubMed: 16648940]

28. Huang Y, Lemieux MJ, Song J, Auer M, Wang DN. Structure and mechanism of the glycerol-3-phosphate transporter from Escherichia coli. Science. 2003; 301(5633):616–20. [PubMed: 12893936]

29. Yin Y, He X, Szewczyk P, Nguyen T, Chang G. Structure of the multidrug transporter EmrD from Escherichia coli. Science. 2006; 312(5774):741–4. [PubMed: 16675700]

30. Vardy E, Arkin IT, Gottschalk KE, Kaback HR, Schuldiner S. Structural conservation in the major facilitator superfamily as revealed by comparative modeling. Protein Sci. 2004; 13(7):1832–40. [PubMed: 15215526]

31. Ho RH, Tirona RG, Leake BF, Glaeser H, Lee W, Lemke CJ, Wang Y, Kim RB. Drug and bile acid transporters in rosuvastatin hepatic uptake: function, expression, and pharmacogenetics. Gastroenterology. 2006; 130(6):1793–806. [PubMed: 16697742]

32. Hofmann K, Stoffel W. Tmbase – A database of membrane spanning protein segments. Biol Chem Hoppe-Seyler. 1993; 374:166.
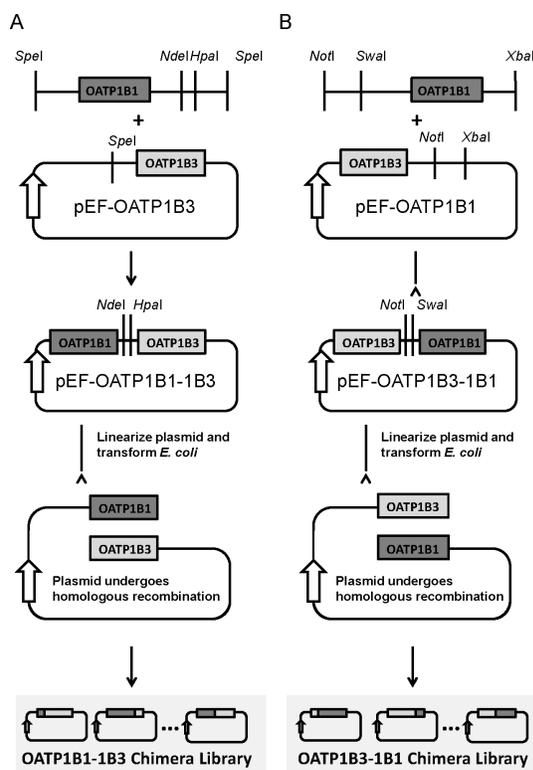
Figure 1. Cloning strategy for OATP1B chimeragenesis
(A) The expression plasmid pEFOATP1B1-1B3 was created by ligating cDNA coding for OATP1B1 into pEF6-OATP1B3 at the *Spe*I restriction site. The unique restriction sites *Nde*I and *Hpa*I allow for linearization of the plasmid prior to transformation and homologous recombination in *E. coli*. (B) The expression plasmid pEF-OATP1B3-1B1 was created by ligating OATP1B1 into pEF6-OATP1B3 between *Not*I and *Xba*I restriction sites in the multiple cloning region. The unique restriction sites *Not*I and *Swa*I allow for linearization of the plasmid prior to transformation and homologous recombination in *E. coli*.

1B1-3 chimera number	amino acid junction	1B3-1 chimera number	amino acid junction
1	12	1	35
2	26	2	101
3	59	3	137
4	127	4	260
5	158	5	317
6	210	6	339
7	230	7	351
8	317	8	394
9	339	9	431
10	402	10	439
11	439	11	481
12	506	12	568
13	534	13	596
14	596	14	608
15	629	15	652
16	641	16	659
		17	672
		18	685

**Figure 2. Identification of regions involved in CCK-8 transport**

OATP1B1-1B3 and OATP1B3-1B1 chimeric constructs were generated by random chimeragenesis, and sequencing determined the exact location of the junction as indicated. In total, 16 OATP1B1-1B3 chimeras and 18 OATP1B3-1B1 chimeras were expressed in HeLa cells and assayed for CCK-8 transport activity. Regions of interest in TM1 (hatched line), TM10 (solid line) and ECL6 (dotted) formed by overlap of regions exhibiting changes in [^{3}H]-CCK-8 transport in both sets of chimeras were identified for further investigation by site-directed mutagenesis. Values are expressed as means ± SEM of n = 5 from at least two independent experiments.
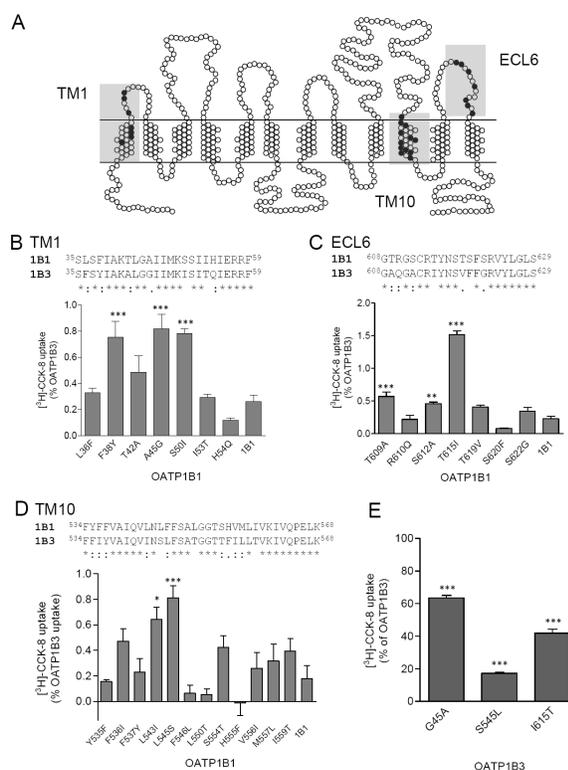
Figure 3. Uptake of [³H]-CCK-8 by cells expressing OATP1B1 and OATP1B3 mutants
(A) Schematic of OATP1B1, including positions of residues mutated in this study. OATP1B1 topology is as predicted by TMPred[32]. Uptake of [³H]-CCK-8 by cells transfected with OATP1B1 mutants in TM1 (B), ECL6 (C), TM10 (D) and OATP1B3 mutants (E) is expressed as % of wildtype OATP1B3 uptake ± SEM, n=4 from two independent experiments. * p < 0.05, ** p < 0.01, *** p < 0.001 relative to wildtype OATP1B1 (B–D) and OATP1B3 (E). Amino acid sequence alignment of OATP1B1 and OATP1B3 in regions of TM1, ECL6 and TM10 formed by overlapping areas of interest as identified by [³H]-CCK-8 uptake by the chimeras.
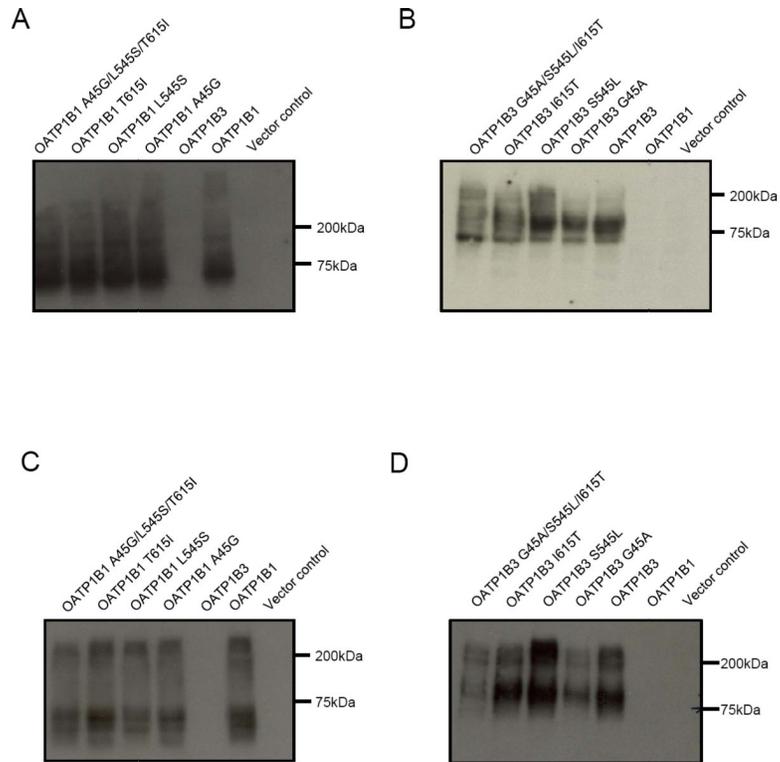
Figure 4. Immunoblot of biotinylated fractions of OATP1B1 and OATP1B3 mutants
Total protein lysates (biotinylated and nonbiotinylated fractions) from Hela cells transfected
with OATP1B1 (A) or OATP1B3 (B) mutants were subjected to SDS-PAGE, transferred to
nitrocellulose and blotted with anti-OATP1B1 or anti-OATP1B3 antibody, respectively.
Cell surface lysates (biotinylated fractions) from Hela cells transfected with OATP1B1 (C)
or OATP1B3 (D) were similarly probed.
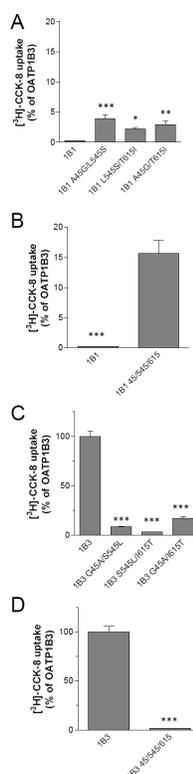
Figure 5. Uptake of [3H]-CCK-8 by cells expressing OATP1B1 double (A) and triple (B) mutants, and OATP1B3 double (C) and triple (D) mutants
Values are expressed as mean % of OATP1B3 wildtype uptake ± SEM, n=4–5 from two independent experiments. ** p < 0.01, *** p < 0.001 relative to wildtype OATP1B1 (A,B) and OATP1B3 (C,D).
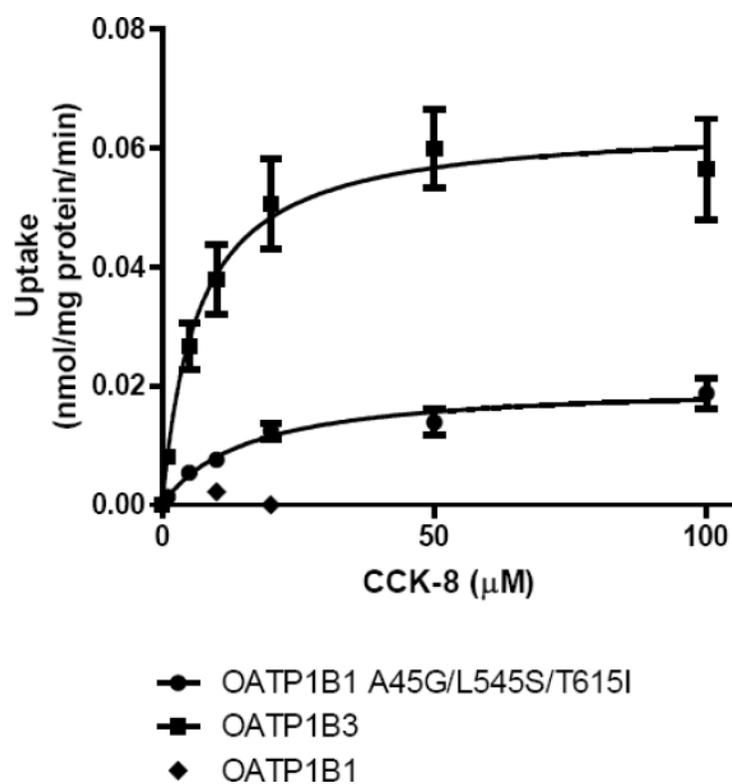
Figure 6. Concentration-dependent uptake of CCK-8 by Hela cells transfected with wildtype OATP1B3 and OATP1B1 A45G/L545S/T615I
Values are expressed as means ± SEM, n = 4 from two independent experiments . Kinetic parameters were obtained by non-linear curve fitting.
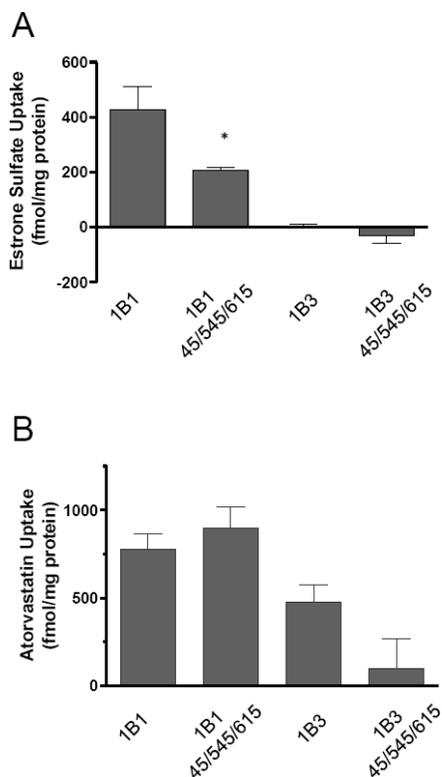
Figure 7. Transport of other OATP1B substrates
(A) Uptake of estrone sulfate by OATP1B1, OATP1B1 A45G/L545S/T615I, OATP1B3 and OATP1B3 G45A/S545L/I615T (B) Uptake of atorvastatin by OATP1B1,OATP1B1 A45G/L545S/T615I, OATP1B3 and OATP1B3 G45A/S545L/I615T. Values are expressed as means ± SEM, n=4 from two independent experiments. * $p < 0.05$ compared to wildtype OATP1B1.
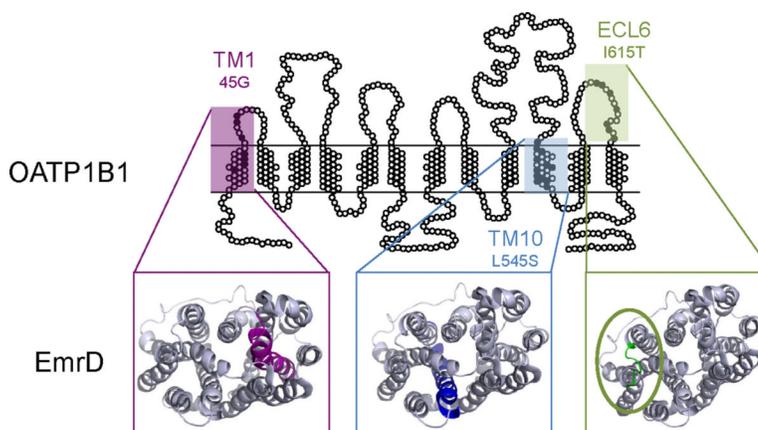
Figure 8. Regions involved in CCK-8 transport by OATP1B1 and OATP1B3, mapped to the crystal structure of the multidrug resistance protein EmrD from *E. coli*[29]
Similar results were obtained for other bacterial protein structures of the major facilitator superfamily, the glycerol-3-phosphate transporter and lactose permease from *E. coli* [28]. Coordinates for the crystal structures were obtained from the Protein Data Bank (www.pdb.org; PDB IDs 2GFP, 1PW4 and 1PV6 respectively). Sequences were aligned using ClustalW with default settings and manually optimized with respect to secondary structure as predicted by TMPred [32]. Figure images were created in Pymol (www.pymol.org).